

The Electromagnetically Induced Transparency in Mechanical Effects of Light

G. S. Agarwal and Sumei Huang

Department of Physics, Oklahoma State University, Stillwater, Oklahoma 74078, USA

(Dated: October 26, 2018)

We consider the dynamical behavior of a nanomechanical mirror in a high-quality cavity under the action of a coupling laser and a probe laser. We demonstrate the existence of the analog of electromagnetically induced transparency (EIT) in the output field at the probe frequency. Our calculations show explicitly the origin of EIT-like dips as well as the characteristic changes in dispersion from anomalous to normal in the range where EIT dips occur. Remarkably the pump-probe response for the optomechanical system shares all the features of the Λ system as discovered by Harris and collaborators.

PACS numbers: 42.50.Gy, 42.50.Wk

Since its original discovery in the context of atomic vapors, electromagnetically induced transparency (EIT) [1–3] has been at the center of many important developments in optical physics [4] and has led to many different applications, most notably in the context of slow light [5–7] and the production of giant nonlinear effects. EIT is helping the progress towards studying nonlinear optics at the single-photon level. EIT has been reported in many other systems [8]. More recently, EIT has been discovered in meta materials [9–12] where resonant structures can be fabricated to correspond to dark and bright modes. Resonators provide certain advantages [13] because by design we can manipulate EIT to produce desired transmission properties of a structure. It would thus be especially interesting to study resonators coupled to other systems such as cavity optomechanical systems. Such nanomechanical systems have attracted considerable interest recently [14–21]. In this letter, we demonstrate the possibility of EIT in the context of cavity optomechanics.

Before discussing our model and results, we set the stage for EIT in cavity optomechanics. As in typical EIT experiments [1–4], for example, in the context of atomic vapors, we need to examine the pump-probe response of a nanomechanical oscillator of frequency ω_m coupled to a high-quality cavity via radiation pressure effects [22, 23] as schematically shown in Fig. 1. Thus, the cavity oscillator of frequency ω_0 and the nano-oscillator interact nonlinearly with each other. The system is driven by a strong pump field of frequency ω_c . This is the coupling field. The probe field has frequency ω_p and is much weaker than the pump field. The mechanical oscillator's damping is much smaller than that of the cavity oscillator. This is very important for considerations of EIT. The decay rate of the mechanical oscillator plays the same role as the decay rate of the ground-state coherence in EIT experiments. The analog of the two-photon resonance condition where EIT occurs would be $\omega_c + \omega_m = \omega_p$. We show how the absorptive and dispersive responses of the probe change by the coupling field and how EIT emerges. We present a clear physical origin of EIT in such a system.

Let us denote the cavity annihilation (creation) operator by c (c^\dagger) with the commutation relation $[c, c^\dagger] = 1$.

The momentum and position operators of the nanomechanical oscillator with mass m are represented by p and q . We also introduce the amplitudes of the pump field and the probe field inside the cavity $\varepsilon_c = \sqrt{2\kappa\varphi_c/(\hbar\omega_c)}$ and $\varepsilon_p = \sqrt{2\kappa\varphi_p/(\hbar\omega_p)}$, where φ_c is the pump power, φ_p is the power of the probe field, and κ is the cavity decay rate. Note that ε_c and ε_p have dimensions of frequency. The optomechanical coupling between the cavity field and the movable mirror can be described by the coupling constant $\chi_0 = \hbar\omega_0/L$, where L is the cavity length. The Hamiltonian describing the whole system reads

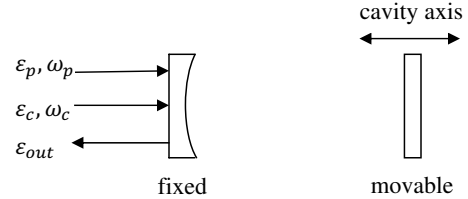


FIG. 1: Sketch of the optomechanical system coupled to a high-quality cavity via radiation pressure effects.

$$H = \hbar\omega_0 c^\dagger c + \left(\frac{p^2}{2m} + \frac{1}{2}m\omega_m^2 q^2 \right) + i\hbar\varepsilon_c (c^\dagger e^{-i\omega_c t} - c e^{i\omega_c t}) + i\hbar(\varepsilon_p c^\dagger e^{-i\omega_p t} - c \varepsilon_p^* e^{i\omega_p t}) - \chi_0 c^\dagger c q. \quad (1)$$

This letter deals with the mean response of the system to the probe field in the presence of the coupling field. Because we deal with the mean response of the system we do not include quantum fluctuations. This is similar to what has been done in the context of EIT work where one uses atomic mean value equations and all quantum fluctuations (due to either spontaneous emission or collisions) are ignored. Thus, we examine the mean value equations, which can be obtained from the Hamiltonian and by addition of the damping terms. We use the factorization assumption $\langle Qc \rangle = \langle Q \rangle \langle c \rangle$ and also transform the cavity field to a rotating frame at the frequency ω_c ,

$\langle c(t) \rangle = \langle \tilde{c}(t) \rangle e^{-i\omega_c t}$. The mean value equations are then given by

$$\begin{aligned} \langle \dot{q} \rangle &= \frac{\langle p \rangle}{m}, \\ \langle \dot{p} \rangle &= -m\omega_m^2 \langle q \rangle + \chi_0 \langle \tilde{c}^\dagger \rangle \langle \tilde{c} \rangle - \gamma_m \langle p \rangle, \\ \langle \dot{\tilde{c}} \rangle &= - \left[\kappa + i \left(\omega_0 - \omega_c - \frac{\chi_0}{\hbar} \langle q \rangle \right) \right] \langle \tilde{c} \rangle + \varepsilon_c + \varepsilon_p e^{-i(\omega_p - \omega_c)t}. \end{aligned} \quad (2)$$

The output field can be obtained by using the input-output relations [24]

$$\varepsilon_{out}(t) + \varepsilon_p e^{-i\omega_p t} + \varepsilon_c e^{-i\omega_c t} = 2\kappa \langle c \rangle. \quad (3)$$

We first note that in the absence of the coupling field, the output field is given by

$$\varepsilon_{out}(t) + \varepsilon_p e^{-i\omega_p t} = \varepsilon_T \varepsilon_p e^{-i\omega_p t} = \frac{2\kappa}{\kappa - i(\omega_p - \omega_0)} \varepsilon_p e^{-i\omega_p t}. \quad (4)$$

The quadratures of the field ε_T , defined by $\varepsilon_T = v_p + i\tilde{v}_p$, show the absorptive and dispersive behavior as a function of the detuning parameter $(\omega_p - \omega_0)$. The field quadratures, as is well known, can be measured by homodyne techniques [24].

Next, we examine the effect of the coupling field. Equations (2) are nonlinear, and therefore the steady-state response contains many Fourier components. We solve in the limit of arbitrary strength of the coupling field; however, we take the probe field to be weak. We specifically are interested in the response of the cavity optomechanical system to the probe in the presence of the coupling field ε_c . Thus, we find the component of the output field oscillating at the probe frequency ω_p . The result of such a calculation is that ε_T is now given by

$$\varepsilon_T = \frac{2\kappa}{d(\delta)} \{ (\delta^2 - \omega_m^2 + i\gamma_m \delta) [\kappa - i(\Delta + \delta)] - 2i\omega_m \beta \}, \quad (5)$$

where

$$d(\delta) = (\delta^2 - \omega_m^2 + i\gamma_m \delta) [(\kappa - i\delta)^2 + \Delta^2] + 4\Delta\omega_m \beta,$$

$$\delta = \omega_p - \omega_c,$$

$$\Delta = \omega_0 - \omega_c - \frac{2\beta\chi_0}{\omega_m},$$

$$\beta = \frac{\chi_0^2 |\tilde{c}_0|^2}{2m\hbar\omega_m},$$

$$\tilde{c}_0 = \frac{\varepsilon_c}{\kappa + i\Delta}. \quad (6)$$

The coupling field has modified the output field at the probe frequency. Note that ε_T is nonperturbative in terms of the strength of the coupling field ω_c . We concentrate on the output field. However, all the results for ε_T also apply to the cavity field at ω_p as the two quantities are proportional to each other.

In order to understand the coupling-field-induced modification of the probe response ε_T , we make reasonable

approximations. We work in the sideband resolved limit $\omega_m \gg \kappa$. This is the limit in which normal mode splitting [20, 21, 25] has been discovered. Because it is known that the coupling between the nano-oscillator and the cavity is strongest whenever $\delta = \pm\omega_m$ or $\delta = \pm\Delta$, the case $\Delta \sim \omega_m$ is considered here. After some simplifications, we can write the output field in an instructive form,

$$\varepsilon_T = v_p + i\tilde{v}_p = \frac{2\kappa}{\kappa - ix + \frac{\beta}{\frac{\gamma_m}{2} - ix}} = \frac{A_+}{x - x_+} + \frac{A_-}{x - x_-}, \quad (7)$$

where $x = \delta - \omega_m$, which is the detuning from the line center. Further, it is seen that the denominator has two roots, which are

$$x_{\pm} = \frac{-i(\kappa + \frac{\gamma_m}{2}) \pm \sqrt{-(\kappa - \frac{\gamma_m}{2})^2 + 4\beta}}{2}, \quad (8)$$

whose nature depends on the power of the coupling laser. For coupling powers less than the critical power

$$\tilde{\varphi}_c = \frac{\hbar\omega_c |\tilde{c}_0|^2 (\kappa^2 + \omega_m^2) (\kappa - \frac{\gamma_m}{2})^2}{8\kappa\beta}, \quad (9)$$

the two roots are purely imaginary. For $\varphi_c > \tilde{\varphi}_c$, the roots are complex conjugates of each other. The region $\varphi_c > \tilde{\varphi}_c$ corresponds to the region where normal-mode splitting [20, 21, 25] occurs and has been studied recently using a very different technique. In the context of optical physics, this is the region where Autler-Townes splitting [26] occurs, although sometimes the distinction between different kinds of splittings is marred. However, for EIT, it is important to have $\gamma_m \ll \kappa$.

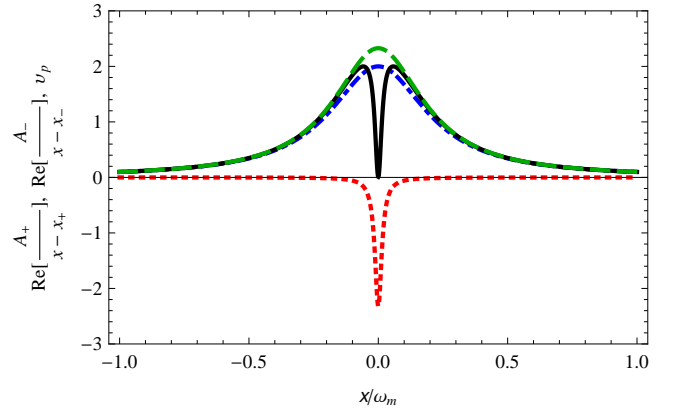


FIG. 2: (Color online) Quadrature of the output field v_p (solid black curve) and the different contributions to it: the real parts of $\frac{A_+}{x-x_+}$ (dotted red curve) and $\frac{A_-}{x-x_-}$ (dashed green curve) as a function of the normalized frequency x/ω_m for input coupling laser power $\varphi_c = 1$ mW. The dot-dashed blue curve is v_p in the absence of the coupling laser.

In order to bring out prominently features like EIT [1–3], we specifically examine the case when the coupling power is less than the critical power. Note that

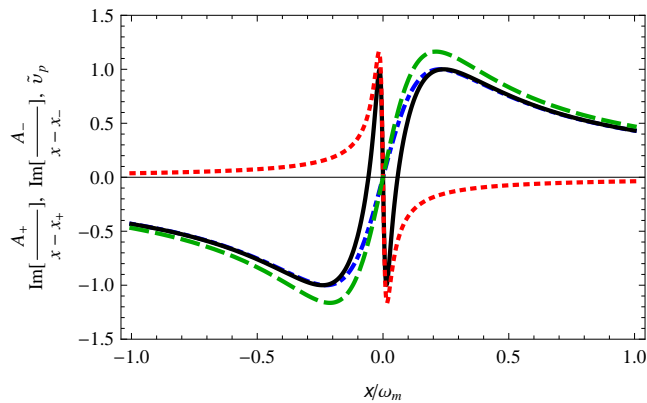


FIG. 3: (Color online) Quadrature of the output field \tilde{v}_p (solid black curve) and the different contributions to it: the imaginary parts of $\frac{A_+}{x-x_+}$ (dotted red curve) and $\frac{A_-}{x-x_-}$ (dashed green curve) as a function of the normalized frequency x/ω_m for input coupling laser power $\wp_c = 1$ mW. The dot-dashed blue curve is \tilde{v}_p in the absence of the coupling laser.

$x_+ \rightarrow -i\frac{\gamma_m}{2}$, $x_- \rightarrow -i\kappa$ as $\beta \rightarrow 0$. Thus, the quadratures of the output field have two distinct contributions in the limit of low values of the coupling laser strength. One contribution is extremely narrow as $\gamma_m \ll \kappa$. This characteristic property leads to the EIT dip. For numerical work, we use parameters from a recent experiment on the observation of the normal-mode splitting [21]: the wavelength of the laser $\lambda = 2\pi c/\omega_c = 1064$ nm, $L = 25$ mm, $m = 145$ ng, $\kappa = 2\pi \times 215$ kHz, $\omega_m = 2\pi \times 947$ kHz, $\gamma_m = 2\pi \times 141$ Hz, the mechanical quality factor $Q = \omega_m/\gamma_m = 6700$. We calculate the critical power $\tilde{\wp}_c$ to be 3.8 mW. In Figs. 2 and 3, we show each contribution in Eq. (7) separately and also the total contribution. We observe that the narrow contribution is inverted relative to the broad contribution, and this leads to the typical EIT-like line shape for the quadrature v_p of the output field. The value at the dip is not exactly zero as $\gamma_m \neq 0$, though the value is very small as $\gamma_m \ll \kappa$. This is similar to what one has in the context of EIT in atomic systems where a strict zero is obtained if the ground-state atomic coherence has an infinite lifetime. In the absence of the coupling field, the narrow feature disappears (blue curve in the Fig. 2). The narrow feature's width has a contribution which depends on the coupling laser power. In leading order, the width is $\frac{\gamma_m}{2} + \frac{\beta}{\kappa}$. For the plot of the Fig. 3, the power-dependent contribution to the width in dimensionless units is $\beta/\kappa^2 \sim 0.065$. The quadrature \tilde{v}_p exhibits dispersive behavior, and the coupling field changes the nature of dispersion from anomalous to normal in the region where quantum interferences are prominent. This behavior of dispersion is similar to the one found by Harris and collaborators in predictions of slow light [5–7] in atomic systems.

We next present the nature of interferences in the region when $\wp_c > \tilde{\wp}_c$ in Figs. 4 and 5. A typical behavior

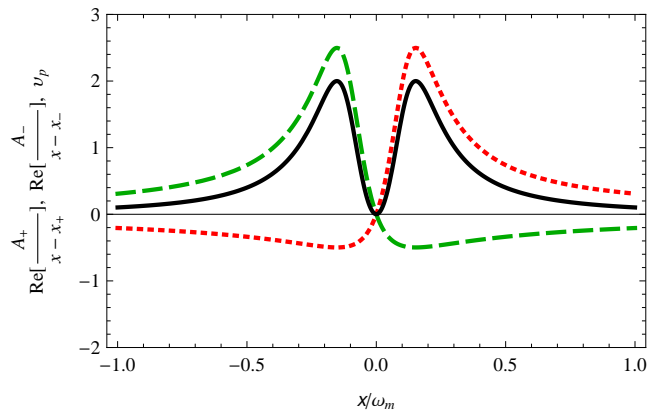


FIG. 4: (Color online) Same as in Fig. 2 except the input coupling laser power $\wp_c = 6.9$ mW and $\wp_c = 0$ case is not shown.

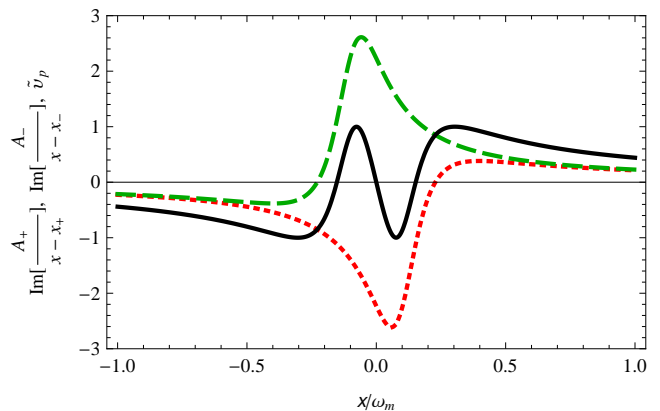


FIG. 5: (Color online) Same as in Fig. 3 except the input coupling laser power $\wp_c = 6.9$ mW and $\wp_c = 0$ case is not shown.

is shown in Fig. 4 which clearly shows how the interference of the two contributions in Eq. (7) leads to the formation of the dip. The two contributions in Eq. (7) lead to asymmetric profiles. In the region of EIT, the tails from these contributions interfere. Unlike the case given by Fig. 2, the two contributions have identical line widths. From Fig. 5, we also see how the dispersive behavior is changed by the coupling field from anomalous to normal in the region where quantum interferences are dominated. The inverted nature of the contribution A_+ should be noted, and it is this which changes the nature of dispersion.

We now explain the origin of the structure (7) for the probe response. Let us re-examine the Hamiltonian (1). Note that we drive the cavity with arbitrary pump field ε_p . This effectively prepares the cavity in a coherent state with a value \tilde{c}_0 if all the other interactions were zero. The trilinear interaction due to radiation pressure $\chi_0 c^\dagger c q$ can now be written as $\chi_0 q |\tilde{c}_0|^2 + \chi_0 q (\tilde{c}_0^* \delta c + \tilde{c}_0 \delta c^\dagger)$ + higher order terms if we write the cavity operator c as $\tilde{c}_0 +$

δc . The pump thus has resulted in a bilinear interaction between the cavity oscillator and the mirror oscillator. The cavity oscillator is driven by the probe field, whereas the matter oscillator has no external drive. The cavity oscillator is damped at the rate κ , whereas the mirror is damped at the rate $\gamma_m \ll \kappa$. This situation typically results [9–13] in line shapes such as (7).

In conclusion, we have shown how an exact analog of EIT can occur in cavity optomechanics when such a system is driven by a weak probe in the presence of a strong

coupling field. We find that the response function for the cavity field at the probe frequency as well as the output field has exactly the same features as the response of a Λ system provided the damping of the nanomechanical mirror is much smaller than the dissipation in the cavity. We further highlighted the interference effects in two distinct regions of the coupling power.

We gratefully acknowledge support from NSF Grant Phys. 0653494.

-
- [1] S. E. Harris, *Phys. Today* **50**, 36 (1997).
 [2] S. E. Harris, J. E. Field, and A. Imamoglu, *Phys. Rev. Lett.* **64**, 1107 (1990).
 [3] K.-J. Boller, A. Imamoglu, and S. E. Harris, *Phys. Rev. Lett.* **66**, 2593 (1991).
 [4] M. Fleischhauer, A. Imamoglu, and J. P. Marangos, *Rev. Mod. Phys.* **77**, 633 (2005).
 [5] L. V. Hau, S. E. Harris, Z. Dutton, and C. H. Behroozi, *Nature (London)* **397**, 594 (1999).
 [6] S. E. Harris, J. E. Field, and A. Kasapi, *Phys. Rev. A* **46**, R29 (1992).
 [7] M. M. Kash, V. A. Sautenkov, A. S. Zibrov, L. Hollberg, G. R. Welch, M. D. Lukin, Y. Rostovtsev, E. S. Fry, and M. O. Scully, *Phys. Rev. Lett.* **82**, 5229 (1999).
 [8] B. S. Ham, M. S. Shahriar, M. K. Kim, and P. R. Hemmer, *Opt. Lett.* **22**, 1849 (1997).
 [9] S. Zhang, D. A. Genov, Y. Wang, M. Liu, and X. Zhang, *Phys. Rev. Lett.* **101**, 047401 (2008).
 [10] N. Papanikolaou, V. A. Fedotov, N. I. Zheludev, and S. L. Prosvirnin, *Phys. Rev. Lett.* **101**, 253903 (2008).
 [11] P. Tassin, L. Zhang, T. Koschny, E. N. Economou, and C. M. Soukoulis, *Phys. Rev. Lett.* **102**, 053901 (2009).
 [12] S. Y. Chiam, R. Singh, C. Rockstuhl, F. Lederer, W. Zhang, and A. A. Bettiol, *Phys. Rev. B* **80**, 153103 (2009).
 [13] D. D. Smith, H. Chang, K. A. Fuller, A. T. Rosenberger, and R. W. Boyd, *Phys. Rev. A* **69**, 063804 (2004).
 [14] C. Genes, A. Mari, P. Tombesi, and D. Vitali, *Phys. Rev. A* **78**, 032316 (2008).
 [15] I. Favero and K. Karrai, *Nature Photonics* **3**, 201 (2009).
 [16] S. Huang and G. S. Agarwal, *New J. Phys.* **11**, 103044 (2009).
 [17] M. Bhattacharya and P. Meystre, *Phys. Rev. Lett.* **99**, 073601 (2007).
 [18] A. Schliesser, R. Rivière, G. Anetsberger, O. Arcizet, and T. J. Kippenberg, *Nature Physics* **4**, 415 (2008).
 [19] M. J. Hartmann and M. B. Plenio, *Phys. Rev. Lett.* **101**, 200503 (2008).
 [20] J. M. Dobrindt, I. Wilson-Rae, and T. J. Kippenberg, *Phys. Rev. Lett.* **101**, 263602 (2008).
 [21] S. Gröblacher, K. Hammerer, M. Vanner, and M. Aspelmeyer, *Nature (London)* **460**, 724 (2009).
 [22] V. B. Braginsky, S. E. Strigin, and S. P. Vyatchanin, *Phys. Lett. A* **287**, 331 (2001).
 [23] V. B. Braginsky, S. E. Strigin, and S. P. Vyatchanin, *Phys. Lett. A* **305**, 111 (2002).
 [24] D. F. Walls and G. J. Milburn, *Quantum Optics* (Springer-Verlag, Berlin, 1994).
 [25] F. Marquardt, J. P. Chen, A. A. Clerk, and S. M. Girvin, *Phys. Rev. Lett.* **99**, 093902 (2007).
 [26] S. H. Autler and C. H. Townes, *Phys. Rev.* **100**, 703 (1955).